Diagnostic value of mammography combined with ultrasound shear wave elastography and magnetic resonance imaging in breast cancer

LONG-XIU QI[1*], XIAO ZHOU[1*], YI-GANG FU[1] and WEN-YAN ZHOU[2]

[1]Department of Radiology, Yancheng No. 1 People's Hospital (The First People's Hospital of Yancheng), Affiliated Hospital of Medical School, Nanjing University, Yancheng, Jiangsu 224000, P.R. China; [2]Department of Ultrasound, Yancheng No. 1 People's Hospital (The First People's Hospital of Yancheng), Affiliated Hospital of Medical School, Nanjing University, Yancheng, Jiangsu 224000, P.R. China

Received July 25, 2024; Accepted November 4, 2024

DOI: 10.3892/ol.2024.14831

Abstract. Breast cancer is one of the most common malignancies affecting women worldwide, and an early diagnosis is critical for improving prognosis. The present study aimed to investigate the diagnostic value of mammography (MG) combined with ultrasound shear wave elastography (SWE) and magnetic resonance imaging (MRI) for the early screening of breast cancer. Patients with breast tumors who underwent lumpectomy at a single hospital between December 2021 and January 2023 were selected and categorized into a benign or malignant group based on pathological findings. All patients had undergone examinations with MG, SWE and MRI. Imaging parameters were subsequently compared between the two groups. A total of 93 patients with breast tumors were included in the study, comprising 37 individuals in the benign group and 56 in the malignant group. MG findings revealed that patients in the malignant group exhibited significantly higher incidences of high breast glandular density, irregular mass margins, unclear mass borders and axillary lymph node involvement compared with those in the benign group. SWE results indicated that the elasticity ratio of the lesion to fat, and the mean and maximum values of the elastic modulus were significantly lower in the benign group than in the malignant group. Additionally, MRI findings demonstrated that the MRI-measured maximum diameter was larger, and the prevalence of irregular lesion morphology, irregular mass margins, signal enhancement and type III time-signal intensity curves was greater in the malignant group compared with the benign group. The diagnostic sensitivity, specificity, positive predictive value and negative predictive value of MG + SWE + MRI were 94.6, 86.5, 91.4 and 91.4%, respectively. Furthermore, the diagnostic efficacy of this combination surpassed that of MG + SWE, MG + MRI and SWE + MRI (area under the curve, 0.906 vs. 0.767, 0.758 and 0.763, respectively). In conclusion, the combination of MG with SWE and MRI exhibits a superior performance in the early diagnosis of breast cancer, exhibiting higher diagnostic accuracy and reliability compared with pairwise combinations.

Correspondence to: Dr Wen-Yan Zhou, Department of Ultrasound, Yancheng No. 1 People's Hospital (The First People's Hospital of Yancheng), Affiliated Hospital of Medical School, Nanjing University, 166 Yulong West Road, Tinghu, Yancheng, Jiangsu 224000, P.R. China
E-mail: 15351554296@163.com

*Contributed equally

Abbreviations: MG, mammography; SWE, shear wave elastography; MRI, magnetic resonance imaging; SE, strain elastography

Key words: breast tumor, radiography, magnetic resonance imaging, shear wave elastography, diagnostic performance

Introduction

Breast cancer is one of the most prevalent malignant tumors among women, with an estimated global incidence of ~2.3 million new cases each year (1). Breast cancer has emerged as a major public health concern, and its incidence is steadily increasing. According to the World Health Organization, breast cancer is the leading cause of cancer-related mortality among women globally; it severely impacts the physical and mental health of patients as well as their quality of life (2). Early detection is primarily achieved through mammography (MG), resulting in a 5-year survival rate of >90% in developed countries. However, in low-income countries, breast cancer is frequently diagnosed at advanced stages, leading to a marked reduction in the 5-year survival rate to <40% (2). Thus, early and accurate diagnosis is crucial for improving the prognosis of patients with breast cancer.

Conventional MG, however, has limitations in early diagnosis (3). The complex anatomical structure of breast tissues and variations in tissue density often hinder the accurate detection of early malignant tumors, particularly those with small diameters or located deep within the breast (4). To address these challenges, new imaging techniques, including ultrasound shear wave elastography (SWE) and magnetic resonance imaging (MRI), have gained considerable attention (5,6).

SWE offers a distinct advantage in characterizing the nature of breast lumps as it quantitatively evaluates the stiffness of tissue and provides objective measurements of elasticity parameters (7) Conversely, MRI delivers extensive information on tissue perfusion and facilitates a comprehensive assessment of lesion morphology, boundaries and internal structure through the dynamic observation of hemodynamic characteristics, which is particularly beneficial for the diagnosis of lesions located deep within the tissue (6).

The primary objective of the present study was to investigate the diagnostic efficacy of a combination of MG, SWE and MRI in the early of detection breast cancer. By comparing the strengths of these imaging techniques in lesion detection, characterization and localization, the study aims to provide an accurate and comprehensive foundation for medical imaging in the early diagnosis of breast cancer. The integration of MG, SWE and MRI may leverage their respective advantages to result in a complementary and comprehensive diagnostic strategy. Through the comparative analysis of different techniques in breast cancer diagnosis, the study aims to provide a reliable and comprehensive diagnostic solution for clinicians, ultimately enhancing the early screening and diagnosis of breast cancer.

Materials and methods

Study design. In the present study, prospective data collection with retrospective analysis was conducted on patients with breast tumors who underwent lumpectomy at Yancheng No. 1 People's Hospital (Yancheng First Hospital, Affiliated Hospital of Nanjing University Medical School; Yancheng, China) from December 2021 to January 2023. Patients were categorized into benign and malignant groups based on histopathology results. Relevant data, including age, medical history, imaging results and lesion characteristics, were systematically collected. The study adhered to the Declaration of Helsinki and was approved by the Ethics Committee of The First People's Hospital of Yancheng (Yancheng, China; approval no. 2021-J-098).

Inclusion criteria. Participants were included based on the following criteria: i) Meeting the diagnostic criteria for breast tumors as outlined in the Chinese expert consensus on the clinical diagnosis and treatment of advanced breast cancer (2021) (8); ii) undergoing lumpectomy at Yancheng No. 1 People's Hospital, with pathological confirmation of breast cancer; iii) being a female aged between 18 and 65 years; and iv) having completed follow-up treatment at Yancheng No. 1 People's Hospital, with comprehensive clinical data available. The exclusion criteria were as follows: i) Prior receipt of surgery, chemotherapy or medication before consultation; ii) pregnancy or lactation; iii) presence of severe pulmonary or cardiac diseases, or abnormal liver or kidney function; iv) coexistence of other diffuse breast lesions; v) implantation of devices such as pacemakers that could be affected by magnetic fields; vi) intolerance to ultrasound contrast agents; vii) presence of breast implants; and viii) lesions with a largest diameter >3 cm.

Study methods

MG. The patients were examined by MG using the Selenia® Dimensions® Digital Mammography System (Hologic, Inc.). Prior to the examination, patients were assessed for contraindications and instructed to remove any external objects that could interfere with the imaging process. Patients were asked to maintain still during the procedure and to position their arms at their sides to facilitate the upward and forward positioning of the breast tissue. The examination utilized an automatic compression system and automatic exposure control system, with exposure settings ranging from 22 to 49 kV for voltage and 4 to 500 mA for current. The image acquisition process complied with the technical standards established by the Chinese Medical Association in 2014 (9) The breasts of the patients were imaged from the mediolateral oblique and bilateral craniocaudal positions, with magnified views and supplementary positions employed as necessary. It was crucial to ensure that the axillary lymph nodes, parasternally located glands and other relevant areas were thoroughly examined to avoid missed diagnoses.

Ultrasound SWE. An AixPlorer Color Doppler Ultrasound machine (SuperSonic Imagine), equipped with a probe operating at frequencies of 4-15 MHz, was utilized for SWE. Patients were positioned supine, with the upper limb on the affected side elevated to fully expose the breast and axillary area. Initially, a 2-dimensional ultrasound examination was conducted to evaluate the morphology and blood flow characteristics of the lesion. The SWE mode was then activated, and the probe was gently placed over the lesion. The size of the sampling frame in the elastic detection area was adjusted until there was no red extrusion mark (a visual indicator signaling that the elasticity measurement exceeds the optimal range of the device) at the top of the frame. This adjustment ensured that the sampling frame adequately covered the lesion and the surrounding area of stiff tissue. For larger lesions extending beyond the sampling frame, multiple sections were measured separately. The part of the lesion exhibiting the highest elasticity value was recorded. Subsequently, patients were instructed to hold their breath for 3 sec. After acquiring a stable image, the elastic parameters of the lesion were recorded, including the maximum value of the elastic modulus (E-max), the mean value of the elastic modulus (E-mean) and the elasticity ratio of the lesion to fat (E-ratio). Each lesion was assessed three times, and the average value was calculated. These parameters were measured by using the Q-Box™ quantification tool (SuperSonic Imagine).

MRI. Dynamic contrast-enhanced (DCE) MRI and diffusion-weighted imaging (DWI) were performed using the MAGNETOM Skyra 3.0T (Siemens AG). The scanning parameters were as follows: For T2-weighted imaging in the axial position, the repetition time (TR)/echo time (TE) values were set at 6,710/75 msec, with 2 excitations and a slice thickness of 4 mm; for T1-weighted imaging in the axial position, the TR/TE values were 630/12 msec, with 2 excitations and a slice thickness of 5 mm; and for DWI, the TR/TE values were set at 3,400/71 msec, with a slice thickness of 5 mm and a b-value of 800 sec/mm^2. For DCE MRI, gadopentetate dimeglumine (Magnevist; Bayer AG) was used as the contrast agent at a dosage of 0.2 ml/kg under high pressure, followed by axial scanning to obtain five sequences. The parameters for this sequence were TR/TE values of 4.66/1.68 msec, with 1 excitation, a slice thickness of 1.6 mm, and an 80-sec interval between each period.

Table I. Analysis of the baseline data of all study subjects.

Parameters	Benign group (n=37)	Malignant group (n=56)	t/χ^2-value	P-value
Age, mean ± SD, years	43.75±9.22	46.42±9.27	-1.362	0.176
Tumor size, mean ± SD, cm	1.72±0.81	3.32±1.45	-6.105	<0.001
Location, n (%)			0.147	0.702
Right	20 (54.05)	28 (50.00)		
Left	17 (45.95)	28 (50.00)		
Tumor shape, n (%)			0.345	0.557
Oval	12 (32.43)	15 (26.79)		
Irregular	25 (67.57)	41 (73.21)		
Growing direction, n (%)			2.890	0.089
Parallel	32 (86.49)	40 (71.43)		
Vertical	5 (13.51)	16 (28.57)		
Mass margin, n (%)			15.171	<0.001
Smooth	21 (56.76)	10 (17.86)		
Irregular	16 (43.24)	46 (82.14)		
Echogenicity, n (%)			29.896	<0.001
Strong	24 (64.86)	6 (10.71)		
Weak	13 (35.14)	50 (89.29)		
Calcification			18.322	<0.001
No	28 (75.68)	17 (30.36)		
Microcalcification	9 (24.32)	39 (69.64)		
Posterior features, n (%)			-	0.517
Enhanced	34 (91.89)	48 (85.71)		
Masked	3 (8.11)	8 (14.29)		

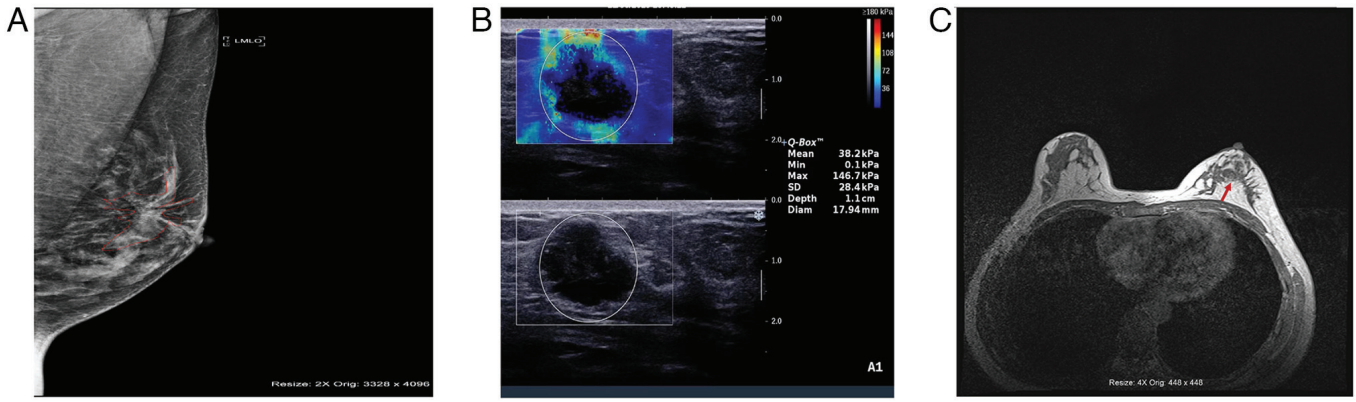

Figure 1. Imaging analysis of breast lesions in different patients using three imaging modalities. (A) Mammography revealing multiple punctate and nodular calcified foci, which are characteristic findings associated with malignancy. (B) Ultrasound shear wave elastography displaying quantitative measurements of tissue stiffness generated using the Q-Box™ quantification tool. (C) Magnetic resonance imaging illustrating lesion morphology and enhancement patterns. The red arrow indicates the lesion in the anterior left breast. LMLO, left mediolateral oblique; Min, minimum; Max, maximum; SD, standard deviation.

Study indicators. The imaging parameters were compared between the benign and malignant groups. This included MG-related parameters, namely breast glandular density, margins, borders and axillary lymph node involvement; SWE-related parameters, namely the E-ratio, E-mean and E-max; and MRI-related parameters, namely the maximum diameter measured by MRI, lesion morphology, mass margins, signal enhancement and time-signal intensity curve (TIC).

Statistical analysis. Data analysis was conducted using SPSS version 20.0 (IBM Corp.). Basic characteristics of the samples were expressed as the mean ± standard deviation. Independent samples t-tests were employed to compare differences in continuous variables between the two groups, while χ^2 or Fisher's exact tests were used for the analysis of categorical variables. The diagnostic efficacy of each of the combinations of MG + SWE, MG + MRI, SWE + MRI and MG + SWE + MRI

Table II. Comparison of imaging parameters.

A, MG

Parameters	Benign group, (n=37)	Malignant group (n=56)	χ^2-value	P-value
Glandular density, n (%)			8.159	0.004
Low	27 (73.0)	24 (42.9)		
High	10 (27.0)	32 (57.1)		
Mass margin, n (%)			8.578	0.003
Smooth	24 (64.9)	19 (33.9)		
Irregular	13 (35.1)	37 (66.1)		
Mass border, n (%)			6.426	0.011
Clear	21 (56.8)	17 (30.4)		
Unclear	16 (43.2)	39 (69.6)		
Axillary lymph nodes, n (%)			6.758	0.009
No	19 (51.4)	14 (25.0)		
Yes	18 (48.6)	42 (75.0)		

B, SWE

Parameters	Benign group, (n=37)	Malignant group (n=56)	t-value	P-value
E-ratio, mean ± SD	3.25±0.92	15.30±2.75	-25.663	<0.001
E-mean, mean ± SD	21.14±8.70	44.42±14.26	-8.888	<0.001
E-max, mean ± SD	99.88±37.07	287.63±89.97	-12.020	<0.001

C, MRI

Parameters	Benign group, (n=37)	Malignant group (n=56)	χ^2/t-value	P-value
MRI-measured maximum diameter, mean ± SD, cm	1.16±0.55	2.06±0.44	-8.724	<0.001
Lesion morphology, n (%)			9.632	0.002
Regular	24 (64.9)	18 (32.1)		
Irregular	13 (35.1)	38 (67.9)		
Mass margin, n (%)			12.580	<0.001
Smooth	29 (78.4)	23 (41.1)		
Irregular	8 (21.6)	33 (58.9)		
Signal enhancement, n (%)			6.241	0.012
Normal	17 (45.9)	12 (21.4)		
Enhanced	20 (54.1)	44 (78.6)		
TIC, n (%)			12.977	0.002
Type I	14 (37.8)	9 (16.1)		
Type II	18 (48.6)	20 (35.7)		
Type III	5 (13.5)	27 (48.2)		

MG, mammography; SWE, shear wave elastography; MRI, magnetic resonance imaging; TIC, time-signal intensity curve; SD, standard deviation.

was assessed, and the sensitivity, specificity, positive predictive value and negative predictive value were calculated. Receiver operating characteristic (ROC) curves were plotted to evaluate the diagnostic accuracy of each combination method and DeLong's test was employed to compare the area under the curve (AUC) values between different diagnostic combinations. To adjust for potential type I errors arising from multiple comparisons among the AUCs, a Bonferroni correction was applied. A significance level of α=0.05 (two-tailed) was considered to indicate statistical significance.

Table III. Results for different combinations of imaging methods for benign and malignant breast tumors and their diagnostic efficacy.

Parameters	Pathological diagnosis, n		Sensitivity, %	Specificity, %	Positive predictive value, %	Negative predictive value, %
	Malignant	Benign				
MG + SWE						
Malignant	39	6	69.6	83.8	86.7	64.6
Benign	17	31				
MG + MRI						
Malignant	41	8	73.2	78.4	83.7	65.9
Benign	15	29				
SWE + MRI						
Malignant	40	7	71.4	81.1	85.1	65.2
Benign	16	30				
MG + SWE + MRI						
Malignant	53	5	94.6	86.5	91.4	91.4
Benign	3	32				

MG, mammography; SWE, shear wave elastography; MRI, magnetic resonance imaging.

Results

Analysis of baseline data. A total of 93 patients with breast tumors were included in the present study, of which 37 patients were in the benign group (mean age, 43.75±9.22 years) and 56 patients were in the malignant group (mean age, 46.42±9.27 years). No significant differences were detected between the two groups regarding age and tumor characteristics, including location, shape, growth direction and posterior features. However, the malignant group exhibited significantly larger tumor sizes (3.32±1.45 vs. 1.72±0.81 cm), as well as a higher percentage of irregular mass margins (82.14 vs. 43.24%), weak echogenicity (89.29 vs. 35.14%) and microcalcification (69.64 vs. 24.32%) compared with the benign group (P<0.001; Table I).

Imaging analysis of typical cases. Typical imaging results from the three techniques in different patients are presented in Fig. 1. The MG image reveals multiple punctate and nodular calcified foci in the left breast, with larger foci located in the central region (Fig. 1A). The SWE results include an E-mean of 38.2 kPa and an E-max of 146.7 kPa, suggestive of malignant lesions (Fig. 1B). An irregular mass in the anterior left breast is revealed by MRI, characterized by inhomogeneous mild-to-moderate enhancement and high-to-low mixed signals, with a greater vascular presence on the anterior side compared with the contralateral side (Fig. 1C).

Comparison of imaging parameters. MG examination results indicated that the malignant group had a greater proportion of cases with high breast glandular density (57.1 vs. 27.0%), irregular mass margins (66.1 vs. 35.1%), unclear mass borders (69.6 vs. 43.2%) and axillary lymph node involvement (75.0 vs. 48.6%) compared with the benign group (P<0.05). SWE results showed that the benign group had significantly lower E-ratio (3.25±0.92 vs. 15.30±2.75), E-mean (21.14±8.70 vs. 44.42±14.26) and E-max values (99.88±37.07 vs. 287.63±89.97) compared with the malignant group (P<0.001). MRI results demonstrated that the malignant group had a larger MRI-measured maximum diameter (2.06±0.44 vs. 1.16±0.55 cm) and a higher proportion of cases with irregular lesion morphology (67.9 vs. 35.1%), irregular mass margins (58.9 vs. 21.6%), signal enhancement (78.6 vs. 54.1%) and Type III TICs (48.2 vs. 13.5%) compared with the benign group (P<0.05; Table II).

Analysis of diagnostic efficacy. The diagnostic sensitivity, specificity and AUC for MG + SWE were 69.6, 83.8 and 0.767% (95% CI, 0.667-0.867), respectively. For MG + MRI, these values were 73.2, 78.4 and 0.758% (95% CI, 0.655-0.860), respectively; for SWE + MRI, they were 71.4, 81.1 and 0.763% (95% CI, 0.661-0.864), respectively; and for MG + SWE + MRI, they were 94.6, 86.5 and 0.906% (95% CI, 0.832-0.979), respectively (Tables III and IV). The diagnostic efficacy of MG + SWE + MRI was significantly superior to that of MG + SWE, MG + MRI and SWE + MRI (P<0.001). However, no significant differences were detected in diagnostic efficacy among the combinations of MG + SWE, MG + MRI and SWE + MRI (Fig. 2, Table IV).

Discussion

The development of breast cancer is influenced by a variety of factors, including heredity, hormone levels and lifestyle choices, and its early diagnosis is challenging due to the complex structure of breast tissue (10). Imaging is crucial in the early screening and diagnosis of breast cancer, and imaging techniques including MG, SWE and MRI are typically used

Table IV. Comparison of the AUCs for different combinations of imaging methods.

Parameters	AUC	95% CI	P-value[a]	P-value[b]	P-value[c]	P-value[d]	P-value[e]	P-value[f]
MG + SWE	0.767	0.667-0.867	0.8533	0.9303	0.0975	<0.001	<0.001	<0.001
MG + MRI	0.758	0.655-0.860						
SWE + MRI	0.763	0.661-0.864						
MG + SWE + MRI	0.906	0.832-0.979						

[a]P-value for MG + SWE vs. MG + MRI; [b]P-value for MG + SWE vs. SWE + MRI; [c]P-value for MG + MRI vs. SWE + MRI; [d]P-value for MG + SWE vs. MG + SWE + MRI; [e]P-value for MG + MRI vs. MG + SWE + MRI; [f]P-value for SWE + MRI vs. MG + SWE + MRI. AUC, area under the receiver operating characteristic curve; MG, mammography; SWE, shear wave elastography; MRI, magnetic resonance imaging.

for the detection of breast cancer during the early stages. Each method has strengths and limitations, particularly in the identification of dense or early-stage lesions, which can impede diagnostic accuracy. Therefore, the present study aimed to elucidate these limitations by exploring the combination of MG, SWE and MRI. The findings indicate that the diagnostic value of this combined approach was superior to that of pairwise combinations, thereby providing a strong foundation for medical imaging in the early screening and diagnosis of breast cancer.

Beyond diagnostic efficacy, the cost-effectiveness of these modalities is crucial for clinical decision-making. MG remains widely accessible and inexpensive, making it a cost-effective first-line screening tool (11). SWE is a newer technique that provides affordable quantitative data on tissue stiffness, which helps to differentiate benign from malignant lesions and potentially reduces unnecessary biopsies for Breast Imaging-Reporting and Data System (BI-RADS) IVa lesions (12). Although MRI is more expensive, it delivers detailed information on vasculature and perfusion, which is valuable for the imaging of complex or dense cases. A previous study suggests that MRI is most cost-effective when used selectively, to complement MG and SWE in challenging scenarios (13). Integrating these methods enhances diagnostic efficacy and helps to manage costs by tailoring modality selection based on patient-specific factors.

Breast density influences the accuracy of diagnostic imaging as dense breast tissue can obscure lesions, thereby reducing the sensitivity of MG. Although MG is a traditional imaging method favored for use in the diagnosis of breast disease due to its simplicity, speed and non-invasive nature, it has notable limitations in detection rates, particularly in cases with high breast glandular density or early lesions (14). Conventional imaging techniques, including MG and ultrasound, often exhibit low sensitivity and specificity, particularly in young patients with dense breast tissue, breast implants or post-surgical scarring (15). Thus, the density of breast tissue continues to pose a challenge to the sensitivity of MG, emphasizing that alternative imaging strategies are necessary (16).

By contrast, SWE is a valuable tool for the quantitative assessment of breast tissue elasticity, allowing for an objective evaluation of tissue stiffness. This technique has shown considerable promise in distinguishing between benign and malignant solid breast masses in previous studies (17-19). MRI

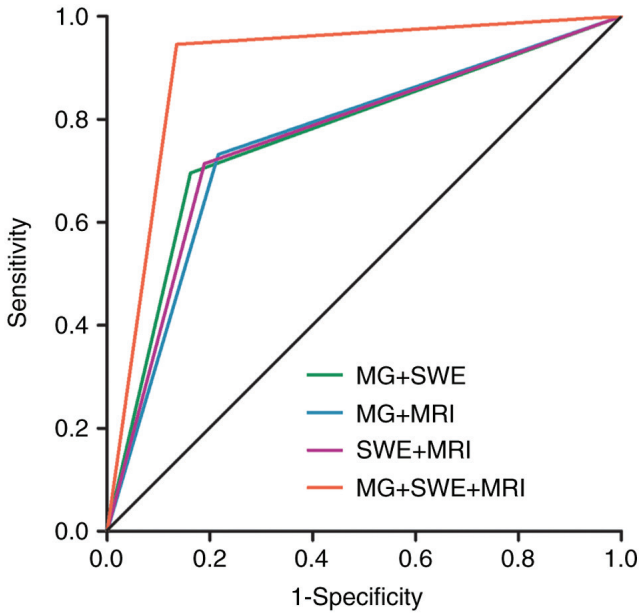

Figure 2. Receiver operating characteristic curves illustrating the diagnostic performance of different imaging combinations. MG, mammography; SWE, shear wave elastography; MRI, magnetic resonance imaging.

complements the aforementioned methods by monitoring the dynamic perfusion processes within lesions, providing essential physiological information about vascular structure, blood flow rate and blood volume. This capability is crucial for determining the blood supply in breast cancer and revealing the physiological status of the lesion. Thus, the integration of MG, SWE and MRI offers a comprehensive and complementary approach for the diagnosis of breast cancer. By addressing the limitations of individual imaging methods, this combined strategy enhances diagnostic accuracy and reliability, ultimately improving the early detection of breast cancer and contributing positively to patient outcomes.

SWE provides quantitative measurements of tissue stiffness in kilopascals by imaging the propagation of transverse waves through tissue. This method enables non-invasive, real-time assessments of tissue elasticity (20). Sravani *et al* (21) investigated the reproducibility of SWE and its alignment with histological findings, which demonstrated its potential for the classification of breast masses as benign or malignant. In contrast to static elastography,

which uses grayscale ultrasound to indicate relative stiffness, SWE offers the advantage of providing objective measurements of lesion stiffness in kilopascals. SWE has shown diagnostic accuracy similar to that of strain elastography (SE) in differentiating between benign and malignant breast lesions. For example, Li *et al* (22) conducted a screening study involving 623 breast lesions, which revealed that SWE and conventional ultrasound exhibited superior diagnostic performance in the diagnosis of cystic solid lesions compared with non-cystic solid lesions. Notably, the threshold for each SWE parameter varied between the cystic and non-cystic lesion groups, being higher in the former group than in the latter. The development of breast cancer is associated with physiological changes, including cell proliferation and neovascularization, which affect the mechanical properties of the tissue. By directly measuring the elastic modulus of tissue, SWE can indirectly provide information on the density and arrangement of tissue cells, thereby reflecting the physiological characteristics of breast cancer (23). Furthermore, Shahzad *et al* (24) concluded that both SE and SWE, when used as supplemental techniques to conventional B-mode breast ultrasound, enhanced the characterization of solid breast lesions and reduced unnecessary biopsies for BI-RADS IVa lesions.

In addition to MG, SWE and MRI, it is important to acknowledge other advanced imaging techniques such as positron emission tomography-computed tomography (PET-CT) and 3-dimensional (3D) MG. PET-CT is primarily used for the detection of metastatic disease, and has limited use in the detection of early breast cancer due to its low resolution for small lesions, as well as its high cost (25). However, it is highly sensitive at detecting metabolically active tumors, which can complement the anatomical and functional data provided by SWE and MRI (26) 3D MG, also known as tomosynthesis, improves detection rates compared with traditional 2D mammography, particularly in women with dense breasts, by providing a detailed, layered view of the breast tissue. However, it does not offer the quantitative or functional insights provided by SWE and MRI (27). Integrating these other modalities may further enhance diagnostic accuracy, particularly in complex cases, although cost-effectiveness and accessibility remain considerations.

In the present study, when MG, SWE and MRI were combined, specific indicators of diagnostic efficacy were evaluated; specifically, the sensitivity, specificity, positive predictive value and negative predictive values were 94.6, 86.5, 91.4 and 91.4%, respectively, with an AUC of 0.906 (95% CI, 0.832-0.979). This demonstrates the high sensitivity and reliability of this combined approach in the accurate diagnosis of breast cancer.

Additionally, the present study examined the differences in diagnostic efficacy among various combinations of imaging techniques. The results indicated that while there were differences in diagnostic efficacy among MG + SWE, MG + MRI, and SWE + MRI, these differences were not statistically significant. Zhang *et al* (28) reported that multiparametric MRI, incorporating DCE-MRI and DWI with apparent diffusion coefficient mapping, enabled accurate breast cancer diagnosis; models using both quantitative and qualitative descriptors from DCE-MRI and DWI exhibited high diagnostic accuracy. Similarly, Yadav *et al* (29) demonstrated that high-resolution DWI, a contrast-free MRI technique, improved lesion detection compared with DCE-MRI. Its diagnostic performance was found to be comparable with that of MRI, suggesting a potentially adjunctive role for high-resolution DWI in conjunction with MG.

The combination of MG, SWE and MRI may offer considerable potential in the personalization of clinical breast cancer management. Each of these imaging modalities provides distinct information about tumor characteristics, which may be beneficial when tailoring an individual treatment plan. For example, MG can be used to detect calcifications and architectural distortions, while SWE offers quantitative data on tissue stiffness that indicates tumor aggressiveness, and MRI provides detailed information on tumor vascularity and perfusion. By combining these modalities, clinicians can obtain a comprehensive profile of the tumor, enabling more precise risk stratification and treatment planning. This integrated imaging approach may be used to inform decisions regarding the necessity of neoadjuvant chemotherapy, the extent of surgical intervention, or the use of targeted therapies, in line with the principles of personalized medicine. Moreover, advanced imaging parameters, such as the elasticity measurements from SWE and the DCE patterns from MRI, could be used to monitor the response to treatment, allowing therapy adjustments to be made on the basis of real-time tumor changes. This approach should not only enhance diagnostic accuracy but also support a more individualized and adaptive treatment strategy, ultimately improving patient outcomes.

The findings of the present study could have translational impact, although further research is required to clarify this. For instance, SWE assesses tissue stiffness, which is associated with the composition of the extracellular matrix (ECM) and the presence of fibrotic tissue. In breast cancer, increased stiffness often arises from collagen deposition and other ECM components, which contribute to tumor progression and metastasis (30). This indicates that SWE can quantitatively measure stiffness, thereby providing indirect information on fibrosis and ECM remodeling within the tumor. Moreover, MRI can capture hemodynamic changes associated with tumor angiogenesis, which is a hallmark of cancer progression (31), and DCE-MRI evaluates vascular permeability and blood flow, reflecting abnormal blood vessel development in the tumor microenvironment. In additional, alterations in perfusion and oxygenation detected by MRI may indicate tumor hypoxia, which promotes aggressive phenotypes and therapy resistance (32). By associating these imaging features with factors within the tumor microenvironment, the combined application of SWE and MRI enhances diagnostic accuracy while offering valuable insights into tumor biology.

The present study had certain limitations that should be considered when interpreting the results. First, the relatively small sample size of 93 cases may affect the generalizability and statistical significance of the findings. Future studies could address this by increasing the sample size through multicenter collaborations to enhance the robustness and external validity of the results. Second, the retrospective nature of the study might have restricted data collection and recording, leading to potential biases. Conducting prospective studies in the future would allow for more

controlled data collection and the opportunity to explore additional clinical variables in real time. Additionally, the present study lacks a separate validation group to confirm the diagnostic performance of the combined imaging modalities due to limitations in sample availability. Future research should address this by including independent validation datasets to confirm the reproducibility of the results and provide stronger evidence for the clinical utility of the multimodal imaging approach in breast cancer diagnosis. Furthermore, as the present study primarily focused on diagnostic performance, the applicability of this combination of imaging techniques for the analysis of long-term follow-up outcomes, such as treatment response and survival rates, requires further investigation. Future research could include longitudinal follow-up studies to evaluate the impact of these imaging modalities on patient outcomes, providing a more comprehensive understanding of their clinical utility in breast cancer management. Lastly, the present study did not explore the biological or physical mechanisms underlying the combined use of MG, SWE and MRI in breast cancer diagnosis. Future research should focus on mechanistic and translational studies to clarify these principles, providing insights into the potential synergies and enhancing understanding of their diagnostic roles.

In conclusion, the combination of MG with SWE and MRI demonstrates a strong performance in the early diagnosis of breast cancer, offering high diagnostic accuracy and reliability. Overall, the present study provides a solid medical imaging foundation for the early screening and diagnosis of breast cancer.

Acknowledgements

Not applicable.

Funding

This study was supported by Yancheng Medical Science and Technology Development Plan Project (grant no. YK2021028).

Availability of data and materials

The data generated in the present study may be requested from the corresponding author.

Authors' contributions

The study was conceived and designed by LXQ, XZ and WYZ. Analysis and interpretation of data was performed by XZ and YGF. The manuscript was drafted by LXQ and XZ, and critically revised for important intellectual content by LXQ, XZ and WYZ. The statistical analysis was performed by LXQ, XZ and YGF. Study supervision was primarily conducted by WYZ, with contributions from all authors. LXQ and XZ confirm the authenticity of all the raw data. All authors read and approved the final version of the manuscript.

Ethics approval and consent to participate

The study complied with the Declaration of Helsinki and was approved by the Ethics Committee of Yancheng No. 1 People's Hospital (approval no. 2021-J-098). All subjects signed a consent form before participation in the study.

Patient consent for publication

Not applicable.

Competing interests

The authors declare that they have no competing interests.

References

1. Kashyap D, Pal D, Sharma R, Garg VK, Goel N, Koundal D, Zaguia A, Koundal S and Belay A: Global increase in breast cancer incidence: risk factors and preventive measures. Biomed Res Int 2022: 9605439, 2022.
2. World Health Organization. Global breast cancer initiative implementation framework: Assessing, strengthening and scaling up of services for the early detection and management of breast cancer: Executive summary. World Health Organization, 2023.
3. Zhu C, Chen M, Liu Y, Li P, Ye W, Ye H, Ye Y, Liu Z, Liang C and Liu C: Value of mammographic microcalcifications and MRI-enhanced lesions in the evaluation of residual disease after neoadjuvant therapy for breast cancer. Quant Imaging Med Surg 13: 5593-5604, 2023.
4. Bodewes FTH, van Asselt AA, Dorrius MD, Greuter MJW and de Bock GH: Mammographic breast density and the risk of breast cancer: A systematic review and meta-analysis. Breast 66: 62-68, 2022.
5. Qi J, Wang C, Ma Y, Wang J, Yang G, Wu Y, Wang H and Mi C: The potential role of combined shear wave elastography and superb microvascular imaging for early prediction the pathological response to neoadjuvant chemotherapy in breast cancer. Front Oncol 13: 1176141, 2023.
6. Zhang L, Zhou XX, Liu L, Liu AY, Zhao WJ, Zhang HX, Zhu YM and Kuai ZX: Comparison of dynamic contrast-enhanced MRI and non-mono-exponential model-based diffusion-weighted imaging for the prediction of prognostic biomarkers and molecular subtypes of breast cancer based on radiomics. J Magn Reson Imaging 58: 1590-1602, 2023.
7. Mao YJ, Lim HJ, Ni M, Yan WH, Wong DW and Cheung JC: Breast tumour classification using ultrasound elastography with machine learning: A systematic scoping review. Cancers (Basel) 14: 367, 2022.
8. Xu B, Hu X, Feng J, Geng C, Jin F, Li H, Li M, Li Q, Liao N, Liu D, *et al*: Chinese expert consensus on the clinical diagnosis and treatment of advanced breast cancer (2018). Cancer 126: 3867-3882, 2020.
9. Chinese Medical Association: Mammography screening and diagnostic consensus. Chin J Radiol 48: 711-717, 2014 (In Chinese).
10. Arian A, Seyed-Kolbadi FZ, Yaghoobpoor S, Ghorani H, Saghazadeh A and Ghadimi DJ: Diagnostic accuracy of intravoxel incoherent motion (IVIM) and dynamic contrast-enhanced (DCE) MRI to differentiate benign from malignant breast lesions: A systematic review and meta-analysis. Eur J Radiol 167: 111051, 2023.
11. Lim YX, Lim ZL, Ho PJ and Li J: Breast cancer in asia: Incidence, mortality, early detection, mammography programs, and risk-based screening initiatives. Cancers (Basel) 14: 4218, 2022.
12. Shen Y, He J, Liu M, Hu J, Wan Y, Zhang T, Ding J, Dong J and Fu X: Diagnostic value of contrast-enhanced ultrasound and shear-wave elastography for small breast nodules. PeerJ 12: e17677, 2024.
13. Abdel Rahman RW, Refaie RMAE, Kamal RM, Lasheen SF and Elmesidy DS: The diagnostic accuracy of diffusion-weighted magnetic resonance imaging and shear wave elastography in comparison to dynamic contrast-enhanced MRI for diagnosing BIRADS 3 and 4 lesions. Egypt J Radiol Nucl Med 52: 185, 2021.
14. Asare B, White MJ and Rossi J: Metaplastic carcinoma with osteosarcomatous differentiation in the breast: Case report. Radiol Case Rep 18: 4272-4280, 2023.
15. Alaref A, Hassan A, Sharma Kandel R, Mishra R, Gautam J and Jahan N: Magnetic resonance imaging features in different types of invasive breast cancer: A systematic review of the literature. Cureus 13: e13854, 2021.

16. Kubota K, Nakashima K, Nakashima K, Kataoka M, Inoue K, Goto M, Kanbayashi C, Hirokaga K, Yamaguchi K and Suzuki A: The Japanese breast cancer society clinical practice guidelines for breast cancer screening and diagnosis, 2022 edition. Breast Cancer 31: 157-164, 2024.
17. Yang H, Xu Y, Zhao Y, Yin J, Chen Z and Huang P: The role of tissue elasticity in the differential diagnosis of benign and malignant breast lesions using shear wave elastography. BMC Cancer 20: 930, 2020.
18. Jiang H, Yu X, Zhang L, Song L and Gao X: Diagnostic values of shear wave elastography and strain elastography for breast lesions. Rev Med Chil 148: 1239-1245, 2020.
19. Suvannarerg V, Chitchumnong P, Apiwat W, Lertdamrongdej L, Tretipwanit N, Pisarnturakit P, Sitthinamsuwan P, Thiravit S, Muangsomboon K and Korpraphong P: Diagnostic performance of qualitative and quantitative shear wave elastography in differentiating malignant from benign breast masses, and association with the histological prognostic factors. Quant Imaging Med Surg 9: 386-398, 2019.
20. Bian J, Zhang J and Hou X: Diagnostic accuracy of ultrasound shear wave elastography combined with superb microvascular imaging for breast tumors: A protocol for systematic review and meta-analysis. Medicine (Baltimore) 100: e26262, 2021.
21. Sravani N, Ramesh A, Sureshkumar S, Vijayakumar C, Abdulbasith KM, Balasubramanian G and Ch Toi P: Diagnostic role of shear wave elastography for differentiating benign and malignant breast masses. SA J Radiol 24: 1999, 2020.
22. Li J, Liu Y, Li Y, Li S, Wang J, Zhu Y and Lu H: Comparison of diagnostic potential of shear wave elastography between breast mass lesions and non-mass-like lesions. Eur J Radiol 158: 110609, 2023.
23. Xie L, Liu Z, Pei C, Liu X, Cui YY, He NA and Hu L: Convolutional neural network based on automatic segmentation of peritumoral shear-wave elastography images for predicting breast cancer. Front Oncol 13: 1099650, 2023.
24. Shahzad R, Fatima I, Anjum T and Shahid A: Diagnostic value of strain elastography and shear wave elastography in differentiating benign and malignant breast lesions. Ann Saudi Med 42: 319-326, 2022.
25. Hadebe B, Harry L, Ebrahim T, Pillay V and Vorster M: The role of PET/CT in breast cancer. Diagnostics (Basel) 13: 597, 2023.
26. Paydary K, Seraj SM, Zadeh MZ, Emamzadehfard S, Shamchi SP, Gholami S, Werner TJ and Alavi A: The evolving role of FDG-PET/CT in the diagnosis, staging, and treatment of breast cancer. Mol Imaging Biol 21: 1-10, 2019.
27. Hodgson R, Heywang-Köbrunner SH, Harvey SC, Edwards M, Shaikh J, Arber M and Glanville J: Systematic review of 3D mammography for breast cancer screening. Breast 27: 52-61, 2016.
28. Zhang M, Horvat JV, Bernard-Davila B, Marino MA, Leithner D, Ochoa-Albiztegui RE, Helbich TH, Morris EA, Thakur S and Pinker K: Multiparametric MRI model with dynamic contrast-enhanced and diffusion-weighted imaging enables breast cancer diagnosis with high accuracy. J Magn Reson Imaging 49: 864-874, 2019.
29. Yadav P, Harit S and Kumar D: Efficacy of high-resolution, 3-D diffusion-weighted imaging in the detection of breast cancer compared to dynamic contrast-enhanced magnetic resonance imaging. Pol J Radiol 86: e277-e286, 2021.
30. Winkler J, Abisoye-Ogunniyan A, Metcalf KJ and Werb Z: Concepts of extracellular matrix remodelling in tumour progression and metastasis. Nat Commun 11: 5120, 2020.
31. Majidpoor J and Mortezaee K: Angiogenesis as a hallmark of solid tumors-clinical perspectives. Cell Oncol (Dordr) 44: 715-737, 2021.
32. Roy S, Kumaravel S, Sharma A, Duran CL, Bayless KJ and Chakraborty S: Hypoxic tumor microenvironment: Implications for cancer therapy. Exp Biol Med (Maywood) 245: 1073-1086, 2020.